SUPPLEMENTARY APPENDIX

Prospective isolation of radiation induced erythroid stress progenitors reveals unique transcriptomic and epigenetic signatures enabling increased erythroid output

Sofie Singbrant,[1] Alexander Mattebo,[1] Mikael Sigvardsson,[2] Tobias Strid[2] and Johan Flygare[1]

[1]Division of Molecular Medicine and Gene Therapy, Lund Stem Cell Center, Lund University and [2]Division of Molecular Hematology, Lund Stem Cell Center, Lund University, Lund, Sweden

 doi:10.3324/haematol.2019.234542

Received: August 14, 2019.

Accepted: January 2, 2020.

Pre-published: January 9, 2020.

Correspondence: *JOHAN FLYGARE* - johan.flygare@med.lu.se

SOFIE SINGBRANT - sofie.singbrant@med.lu.se

Supplementary Appendix

Supplemental Methods

Mice and transplantations

Mice were bred and maintained at the BMC animal facilities, Lund University, Sweden, or obtained from Taconic Biosciences. All procedures involving mice were approved by the Animal Ethics Committee of Malmö/Lund, Sweden.

Anemia was induced by subjecting 8-12w-old recipient mice (C57Bl/6; Ly5.2) to a split dose of lethal irradiation of 2x500 cGy, followed by bone marrow (BM) transplantation to rescue and trigger stress-erythropoiesis. $2x10^6$ unfractionated BM cells from B6SJL (Ly5.1) donors with or without Kusabira Orange (KuO; kindly provided by Dr. Hiromitsu Nakauchi) were transplanted intravenously (i.v.) by tail vein injection. Recipients were sacrificed on day 8 for analysis of stress recovery in the spleen.

For analysis of spleen colony formation (CFU-S8) 600 FACS-sorted cells of each stress-progenitor population from day8 stressed spleens were transplanted i.v. into lethally irradiated secondary recipients without support, and scored for macroscopic CFU-S colonies 8 days later after 2 hour fixation in Bouin's solution (Sigma-Aldrich Sweden, Stockholm, Sweden) and two washings in 70% EtOH (Apoteket, Lund, Sweden).

For *in vivo* tracing, KuO+ stress-progenitor populations were FACS-sorted from day8 stressed spleens, and 500 sMPPs, 5000 sBFU-Es or 5000 sCFU-Es were transplanted i.v. into lethally irradiated secondary recipients together with 10^5 unfractionated wild-type BM cells as support. Secondary recipients were bled at 1, 2 and 4 weeks, and sacrificed at 2 or 4 weeks post transplantation for analysis of lineage potential and kinetics in peripheral blood (PB), BM and spleen.

To analyze the BMP-dependence of stress progenitors, $0.75x10^6$ unfractionated BM cells from BMPRII conditional knock out mice (BmprIIfl/fl Vav-Cre) or wildtype littermate controls (BmprIIfl/fl Cre negative) were competitively transplanted at a 1:1 ratio with KuO+ wildtype BM and analyzed on day 8 for stress recovery in the spleen.

Cell preparations and flow cytometry

Bone marrows (BM) and spleens were homogenized and filtered to single cell suspensions. For lysis of RBCs, peripheral blood (PB) was resuspended 2x2 minutes in room temperatured ammonium chloride (Stemcell Technologies, Cambridge, UK). For the initial colony forming experiment with CD150 alone (Fig. 1A), cells were c-Kit enriched using CD117 MicroBeads kit (Miltenyi Biotec, Lund, Sweden) prior to FACS-sorting. In all other experiments, except for analysis of BMP-dependence where mononuclear spleen progenitors instead were enriched using Lymphoprep (1.077 g/ml, Fresenius Kabi, Oslo, Norway), the initial enrichment for progenitors was carried out by lineage depletion using unconjugated antibodies produced in rat against murine B220, CD4, CD8, Gr-1 and Ter-119 (all from BioLegend, San Diego, CA, USA). Lineage-positive cells were removed with a magnetic particle concentrator (MPC-6; ThermoFisher Scientific, Göteborg, Sweden) and sheep anti-rat Fc-conjugated immunomagnetic beads (ThermoFisher Scientific).

For determination of PB reticulocyte and platelet levels, whole PB was resuspended in BD Retic-Count (BD Biosciences, Stockholm, Sweden) and analyzed with flow cytometry according to standard protocol.

For flow cytometry analysis and sorting, the following antibodies against murine epitopes were used: Screening for new markers for stress-erythroid progenitors; CD71 (FITC; BioLegend), CD9 (PE, clone MZ3; BioLegend), CD48 (PE, BioLegend), CD63 (PE, BioLegend), CD79b (PE, BioLegend), CD34 (PE, BD Biosciences), CD11a (PE, BioLegend), CD24a (PE-Cy7, clone M1/69; BioLegend), CD150 (Biotin, clone TC15-12F12.2; BioLegend), c-Kit (APC780; eBioscience/ThermoFisher Scientific, Göteborg, Sweden), Sca1 (BV421; BioLegend), B220 (PE-Cy5; BioLegend), CD3 (PE-Cy5; BD Biosciences), Gr-1 (PE-Cy5; BioLegend) and Ter-119 (PE-Cy5; BioLegend), sorting of stress-erythroid progenitor populations and analysis of liquid cultures; CD71 (FITC; BioLegend or biotin; BD Biosciences), CD9 (PE or FITC, clone MZ3; BioLegend), CD24a (PE-Cy7, clone M1/69; BioLegend), CD150 (APC, clone TC15-12F12.2; BioLegend), CD133 (PE, clone 315-2C11; BioLegend), c-Kit (APC780; eBioscience/ThermoFisher Scientific), Sca1 (BV421; BioLegend), B220 (Biotin or PE-Cy5; BioLegend), CD3 (Biotin or PE-Cy5; BD Biosciences), Gr-1 (Biotin or PE-Cy5; BioLegend) and Ter-119 (Biotin or PE-Cy5; BioLegend), *in vivo* tracing of Meg/E differentiation potential in PB, BM and spleen; CD41 (FITC), CD45.1 (PE-Cy7; BioLegend), Ter-119 (APC; BioLegend) and CD71 (Biotin; BD Biosciences),

in vivo tracing of B/T/M differentiation potential in PB, BM and spleen; B220 (FITC and APC; BioLegend), Gr-1 (FITC; BioLegend), CD45.1 (PE-Cy7) and CD3 (APC; BioLegend), sorting of steady-state progenitors; B220 (PE-Cy5), CD3 (PE-Cy5), Gr-1 (PE-Cy5), Ter-119 (BV510; BioLegend), c-Kit (APC780; eBioscience), Sca1 (BV421; BioLegend), FcgR (APC; BioLegend), CD41 (BV605; BD Bioscience), CD105 (Biotin; Clone BioLegend) and CD150 (PeCy7; clone TC15-12F12.2; BioLegend). All biotinylated antibodies were detected with Streptavidin-conjugated Qdot605 (ThermoFisher Scientific), except for the sorting of steady-state progenitors, where Qdot655 (Life Technologies/ThermoFisher Scientific, Göteborg, Sweden) was used instead. Fc receptor block (BD Biosciences) was used for sorting samples, and dead cells were excluded using 7-aminoactinomycin D (7-AAD; Sigma-Aldrich Sweden, Stockholm, Sweden) or 4',6-diamidino-2-phenylindole (DAPI; ThermoFisher Scientific). Flow cytometry analyses were performed on BD FACS Canto II, LSR II or Fortessa (Becton Dickinson, Stockholm, Sweden). Fluorescence activated cell sorting (FACS) was performed on BD FACS Aria IIu or Aria III (Becton Dickinson). Results were analyzed with FlowJo 8 software (Tree Star, Ashland, OR, USA).

Hematopoietic progenitor assays

FACS-sorted stress- and steady-state progenitor populations were plated in methylcellulose (M3236; Stemcell Technologies, Cambridge, UK) supplemented with 1% Penicillin/Streptomycin (P/S; Nordic Biolabs, Täby, Sweden) and 50 ng/ml mSCF (PeproTech Nordic, Stockholm, Sweden), 5 U/ml hEPO (Apoteket) and 100 nM Dexamethasone (Sigma-Aldrich Sweden) or 5 U/ml hEPO alone for erythroid progenitor colonies (BFU-Es, CFU-Es), alternatively 50 ng/ml mSCF, 5 U/ml hEPO, 10 ng/ml mIL-3 (PeproTech Nordic), 50 ng/ml hIL-6 (PeproTech Nordic) and 50 ng/ml hTPO (PeproTech Nordic) for mixed colonies (multi, myeloid, MegE, mature erythroid). 100 nM Dexamethasone was added to erythroid cultures in order to increase the size of BFU-Es and facilitate accurate BFU-E scoring[1]. All colony assays were incubated at 37°C incubators in 5% CO_2 with either 21% or 1-4% O_2 as indicated, and scored on day 4 (CFU-Es) or 7-8 (BFU-Es and mixed colonies).

Sorted sMPPs were also plated in liquid culture; SFEM (Serum-Free Expansion Media; Stemcell Technologies) supplemented with 1% P/S, 50 ng/ml mSCF, 5 U/ml

hEPO, 10 ng/ml mIL-3, 50 ng/ml hIL-6 and analyzed by flow cytometry for changes in surface marker expression.

Morphology

KuO contribution in whole spleens of secondary recipients was assessed by epifluorescence microscopy using bright field illumination and green filtered laser excitation on an IX70 microscope (Olympus Sverige, Solna, Sweden) equipped with a DP72 camera (Olympus Sverige), 4x objective lens (UPlanFl 4x; Olympus Sverige) and a Lumen200 laser (Prior Scientific Instruments, Cambridge, UK). The pictures were assembled using the Manual Multiple Image Alignment tool on the CellSens Standard software (version 1.6; Olympus Sverige).

RNA sequencing and bioinformatics

Gene expression data from RNA sequencing comparing erythroid progenitor populations from murine embryonic day 14.5-15.5 fetal liver has previously been described[1], and is deposited in the NCBI's Gene Expression Omnibus[2] under GEO Series accession number GSE26086.

For transcriptional profiling of splenic stress- and BM steady-state progenitors, cells were sorted in triplicates (660-760 cells/sample of sMPPs; $CD150^{+}CD9^{+}Sca1^{+}$, 3000 cells/sample of sBFU-Es; $CD150^{+}CD9^{+}Sca1^{-}$: 3000 cells/sample of sCFU-Es; $CD150^{+}CD9^{-}$ or 1000 cells/sample of steady-state BFU-Es; $CD150^{+}CD9^{+}Sca1^{-}$, all populations within $Lin^{-}Kit^{+}CD71^{low}CD24a^{low}$ cells). Total RNA was isolated using RNeasy micro kit (Qiagen, Sollentuna, Sweden) and RNA quality was controlled using Agilent RNA 6000 Pico Kit (Agilent Technologies Sweden, Kista, Sweden). Strand specific RNA-seq libraries were constructed using SMARTer Stranded Total RNA-Seq Kit v2 (Pico Input Mammalian; Takara Bio USA, Mountain View, CA, USA) followed by sequencing on a HiSeq3000 (Illumina, San Diego, CA, USA) by the UCLA Technology Center for Genomics & Bioinformatics.

The resulting Fastq files were aligned to mouse reference genome (mm10) using STAR[3] on the Galaxy platform (https://usegalaxy.org/), and the resulting bam files were analyzed further using the HOMER platform[4]. Initial Tag-directories were constructed using *makeTagdirectory* with option *-flip*. Expression matrixes were created using *analyzeRepeats.pl* with settings *mm10 rna* and options *-count exons, -condeseGenes* and *-rpkm* for normalized expression or *-noadj* for files for

downstream statistical analyses. Statistically different expressed genes were identified using the created raw expression matrix with genes, with less than a mean of 50 raw tags in at least one sample filtered out, and the command *getDiffExpression.pl* using *DESeq2*[5] as statistical tool.

The heatmap in Figure 3 displays genes with significant differential expression between any of the samples (FDR<0.05, log2FoldChange>0.58) from RNA-sequencing of FACS sorted stress-progenitor populations. RPKM values +1 were imported to Cluster3[6] and adjusted by log transformation and center genes on mean, followed by hierarchical clustering using average linkage with uncentered correlation, and visualizing in Java Treeview[7]. Gene lists from generated heatmap clusters were also used for gene set enrichment analysis (GSEA) by *MSigDB* (collections *H, C1, C2, C3, C5)* and overlaps were calculated for an FDR <0.05[8, 9].

Differentially expressed genes between steady-state and stress-BFU-Es (-log10FDR>2, log2FoldChange>0.58) were sorted into a pre-ranked gene list based on fold change values, then analyzed by the *GSEAPreranked* software[8, 10] (gene set = C2.all.v6.2.symbols.gmt and *nperm* = 1000), and results were displayed as enrichment plots.

The generated RNA-seq data discussed in this publication have been deposited in NCBI's Gene Expression Omnibus[2] and are accessible through GEO Series accession number GSE139336.

Assay for Transposase Accessible Chromatin sequencing

3000 stress- and steady-state BFU-Es were sorted in triplicates ($Lin^-Kit^+CD71^{low}CD24a^{low}CD150^+CD9^+Sca1^-$ for both populations) from murine steady-state BM and day8 stressed spleen respectively. Sorted cells were washed in ice cold PBS (HyClone Phosphate Buffered Saline; GE Healthcare Life Sciences, Marlborough, MA, USA) prior to Assay for Transposase Accessible Chromatin (ATAC) library preparation as described previously[11]. Libraries were subject to 76 cycles of single-end sequencing on a NextSeq500 (Illumina). The data was mapped to mm10 using Bowtie2 with default settings[12] on the Galaxy platform (https://usegalaxy.org/). For ATAC-peak finding, bam files mapped to mm10 were processed by the ENCODE ATAC-seq pipeline (https://github.com/kundajelab/atac_dnase_pipelines) (*-species mm10, -enable_idr, -no_xcor*). Optimal Irreproducible Discovery Rate (IDR) peaks were used for

downstream analyses. Additional analyses were performed using the HOMER platform[4]. Tag directories (*makeTagDirectory with default settings)* with reads mapped to the mitochondrial chromosome filtered out were initially created. Peak-files with peaks from BM and Spleen samples merged were created using *mergePeaks.pl*. Abundance of ATAC-tags on peak positions was analyzed on merged ATAC-seq tag directories from triplicates with peak size estimate set to 175 bp. For histograms the *annotatePeaks.pl* with the options *mm10, -size 5000 -hist 25 -d* [path to tag directories] command using normalization to 10M mapped reads (default) and files for heatmap visualization using the *annotatePeaks.pl* as before, but with the addition of option *-ghist* command, was used. Clustering of heatmaps was performed using Cluster3[6] (K-means clustering, 3 clusters 100 runs, of the ATAC-seq signal in accessible regions, merged from triplicates) and visualized in Java Treeview[7].

The generated ATAC-seq data discussed in this publication have been deposited in NCBI's Gene Expression Omnibus[2] and are accessible through GEO Series accession number GSE139336.

Statistical analysis

For all statistical analysis, apart from RNA- and ATAC sequencing where specifics are stated, significance has been calculated using ANOVA accounting for multiple comparisons, followed by Tukey's multiple comparisons test. One-way ANOVA was used for single time point analysis and Two-way ANOVA was used when measuring potential over time (Figure 2). *P≤0.05, **P≤0.01, ***P≤0.001, ****P≤0.0001.

A

Gene	BFU-E	CFU-E	Ter119	Ter119/BFU-E (>10x)
CD24a	24.67	191.52	1 546.88	62.7
CD82	13.07	45.93	356.30	27.3
Gene	**BFU-E**	**CFU-E**	**Ter119**	**BFU-E/CFU-E (>10x)**
CD9	15.51	0.98	0.38	15.8
CD11a	34.60	0.31	0.60	11.1
CD34	13.54	0.21	0.39	65.1
CD48	27.29	1.54	0.40	17.7
CD63	14.57	1.07	0.63	13.6
CD79b	8.60	0.07	0.38	122.9

B

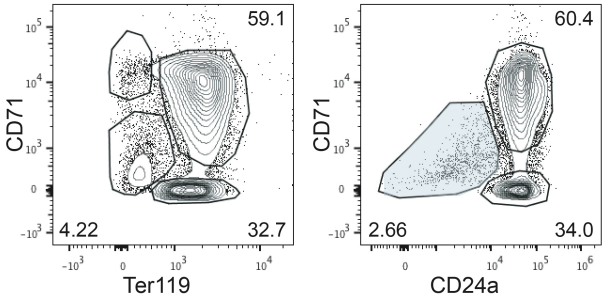

C

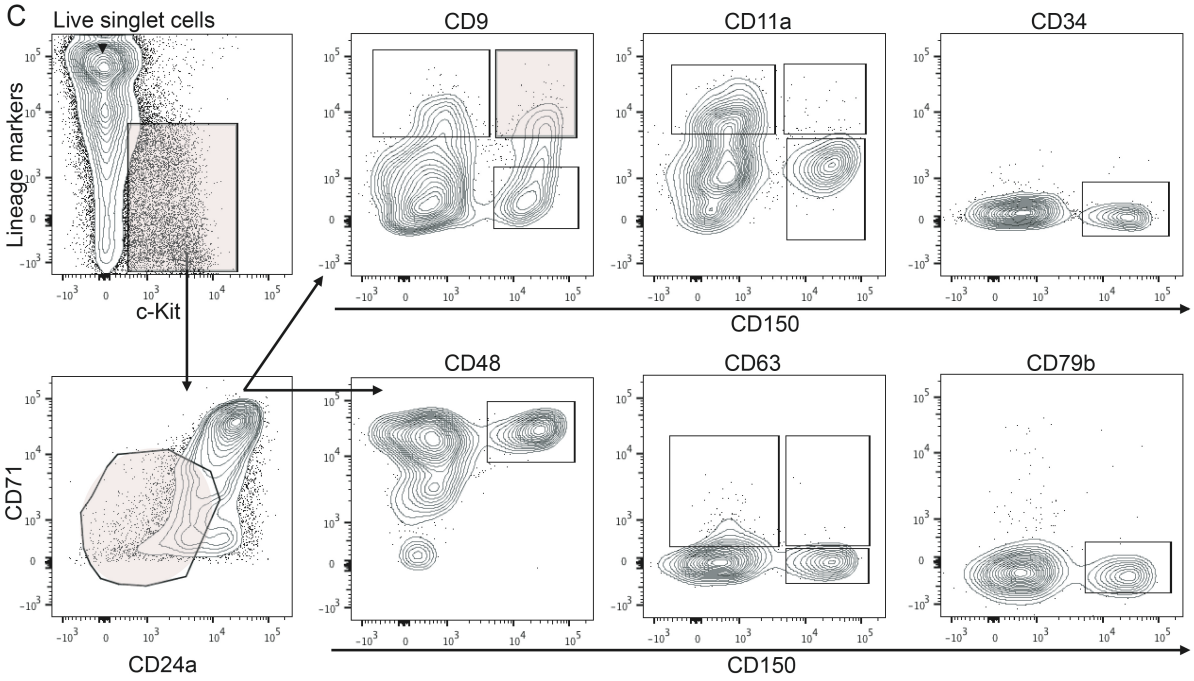

Supplemental Figure 1. Identification of CD9 as a novel marker of stress BFU-Es.

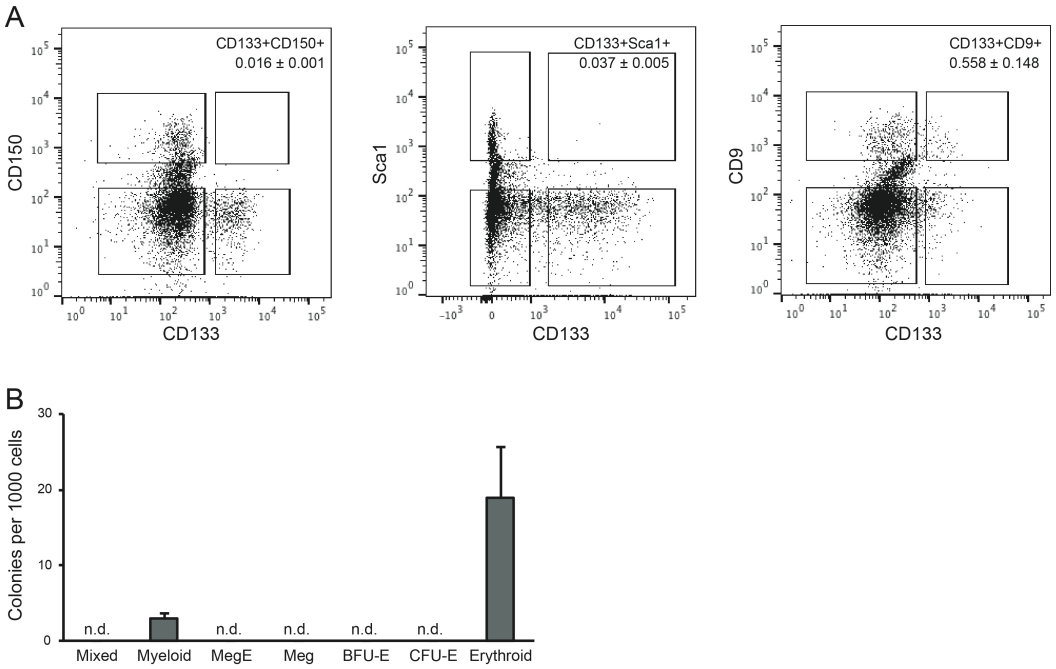

Supplemental Figure 2. CD133 expression does not overlap with CD150+, and does not mark stress BFU-E potential.

A

	% of whole PB	sCFU-Es	sBFU-Es	sMPPs	sBFU-Es vs sCFU-Es	sBFU-Es vs sMPPs
1w	RBCs	98,08 +/- 0,57	98,65 +/- 0,08	98,9 +/- 0,17		
	Retics within RBC	0,19 +/- 0,01	0,36 +/- 0,03	0,14 +/- 0,00	****	****
	Platelets	1,83 +/- 0,57	1,28 +/- 0,08	1,01 +/- 0,17		
2w	RBCs	84,35 +/- 1,44	88,53 +/- 1,08	88,07 +/- 0,80	**	
	Retics within RBC	2,60 +/- 0,55	5,33 +/- 0,39	2,86 +/- 1,16	**	
	Platelets	15,42 +/- 1,48	11,26 +/- 1,10	11,82 +/- 0,79	**	
4w	RBCs	96,40 +/- 1,23	96,93 +/- 0,37	98,40 +/- 0,36	**	
	Retics within RBC	28,22 +/- 8,67	15,99 +/- 4,19	14,16 +/- 3, 69		
	Platelets	2,30 +/- 0,71	2,27 +/- 0,47	1,16 +/- 0,30		

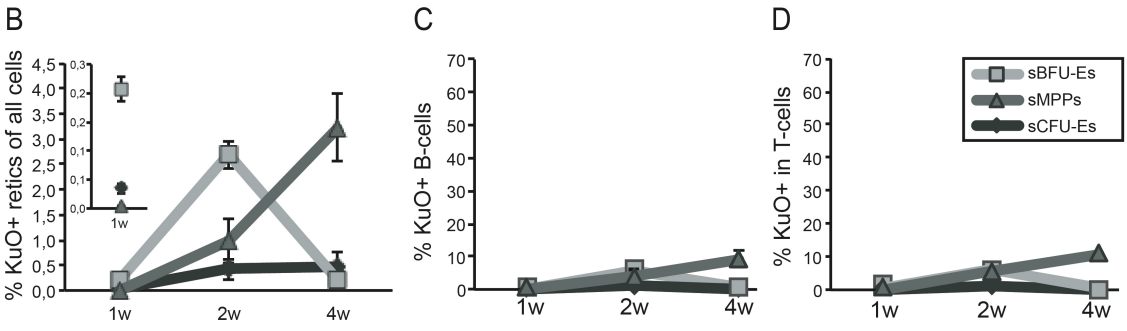

Supplemental Figure 3. In vivo repopulation potential and kinetics of isolated splenic day 8 stress progenitors in peripheral blood.

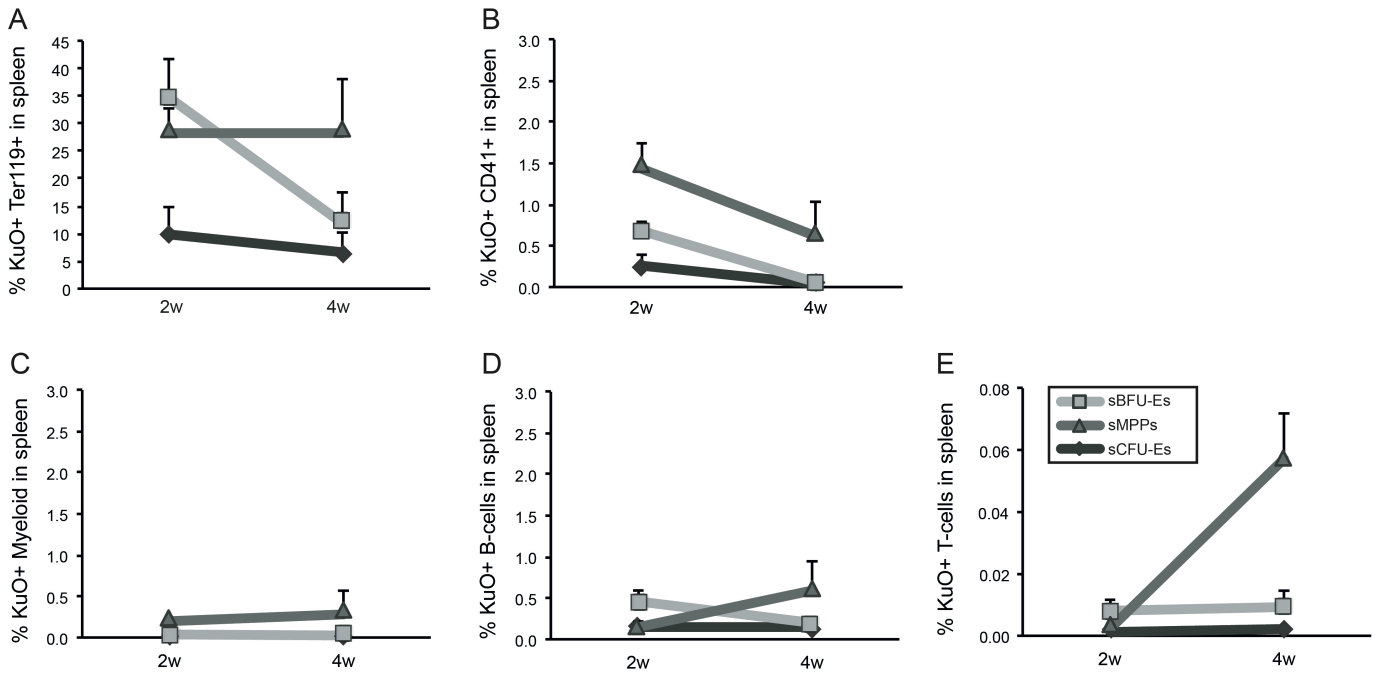

Supplemental Figure 4. In vivo repopulation potential and kinetics of early progenitors in spleen.

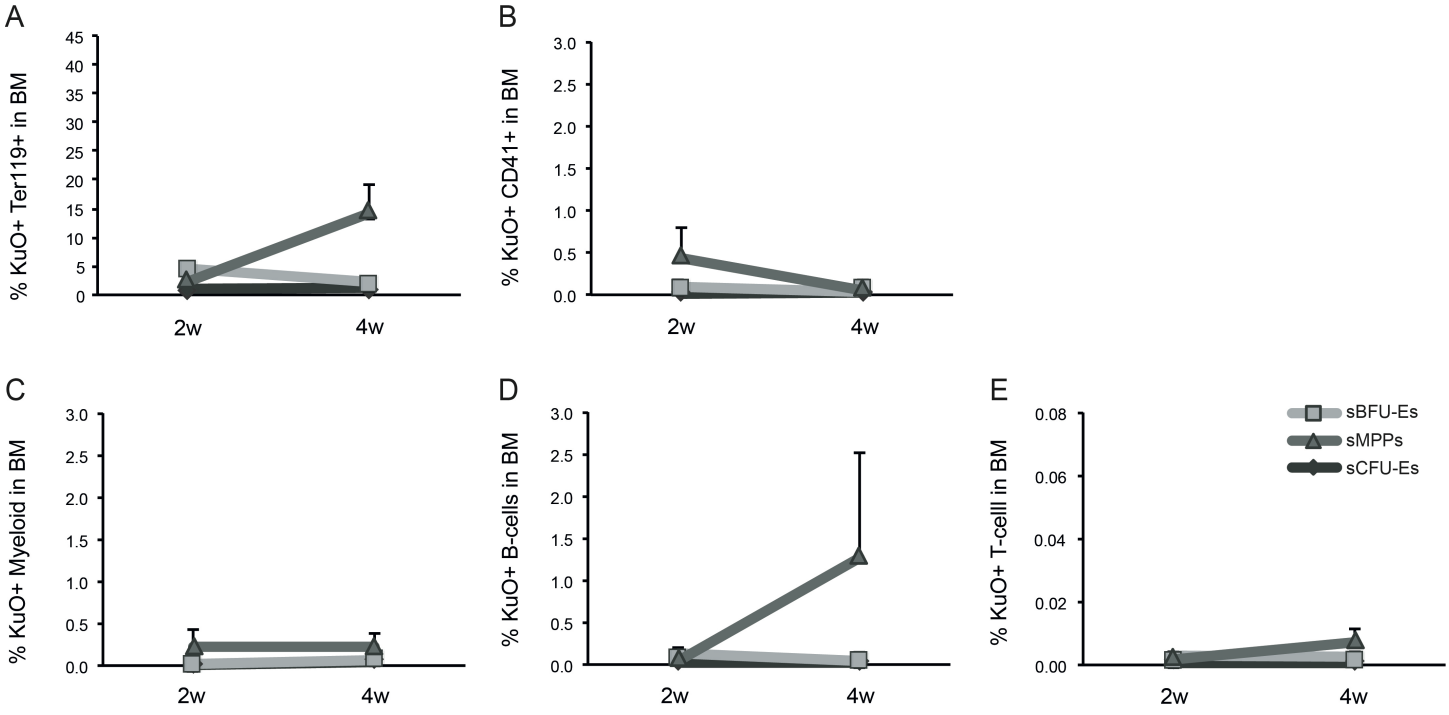

Supplemental Figure 5. In vivo repopulation potential and kinetics of early progenitors in bone marrow.

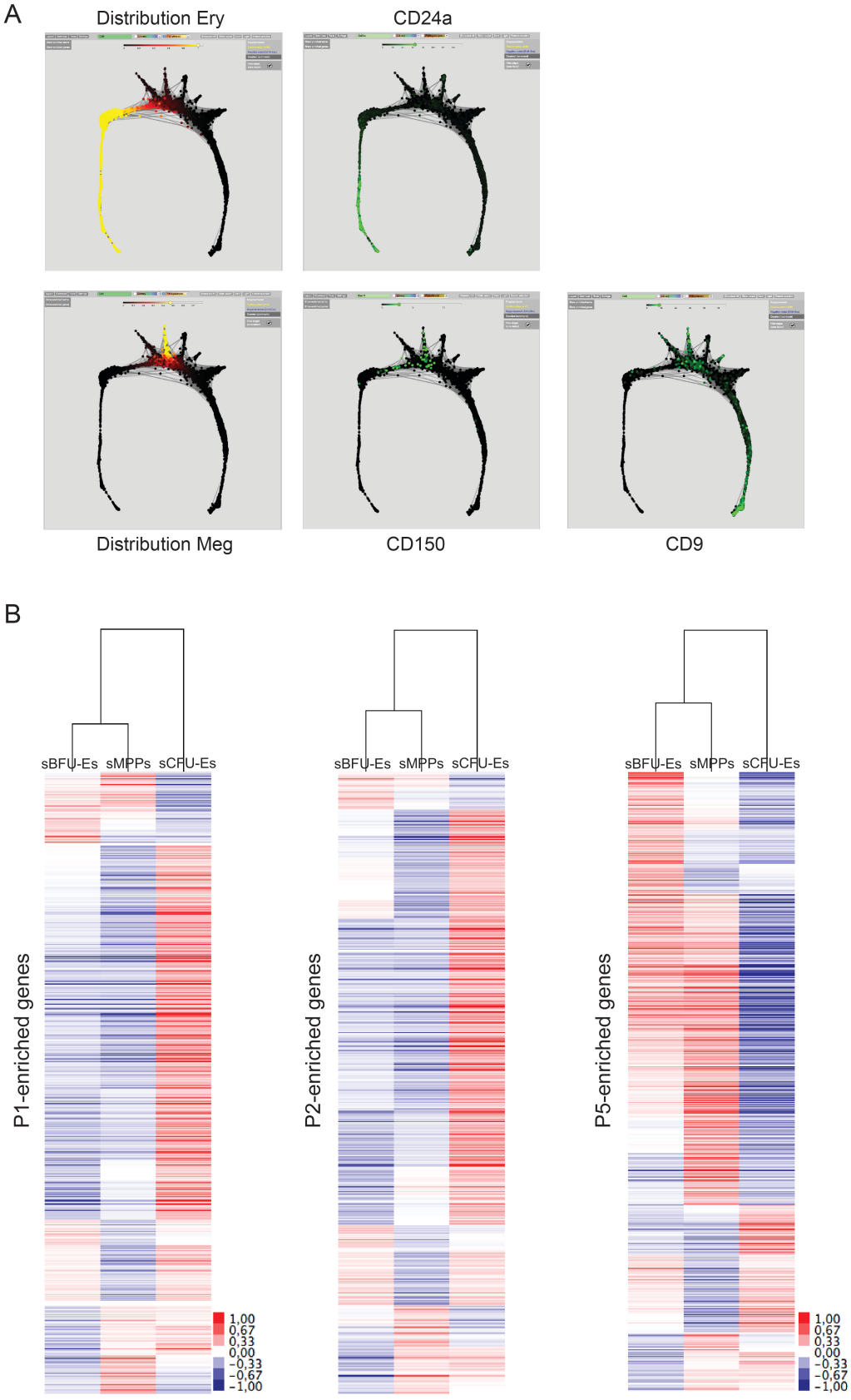

Supplemental Figure 6. Splenic stress progenitors map closely with their steady-state bone marrow counterparts.

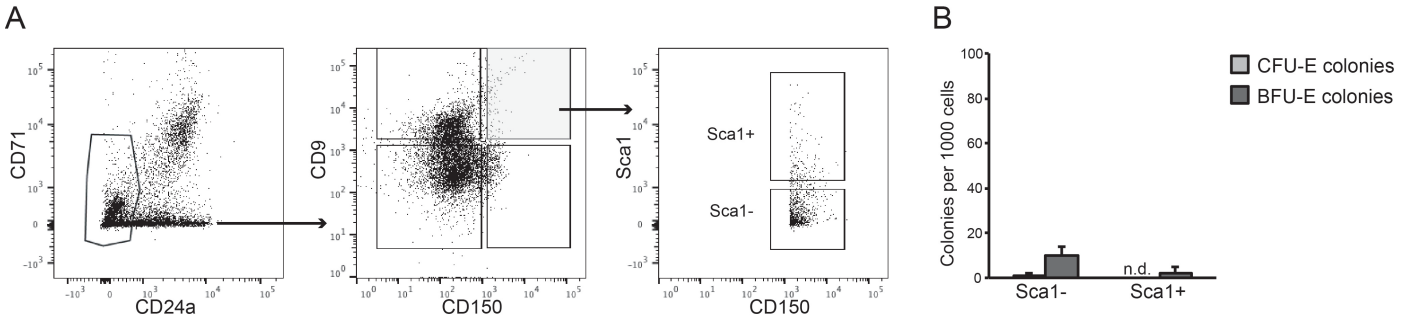

Supplemental Figure 7. Only low levels of BFU-E-forming progenitors are found in the spleen during steady-state.

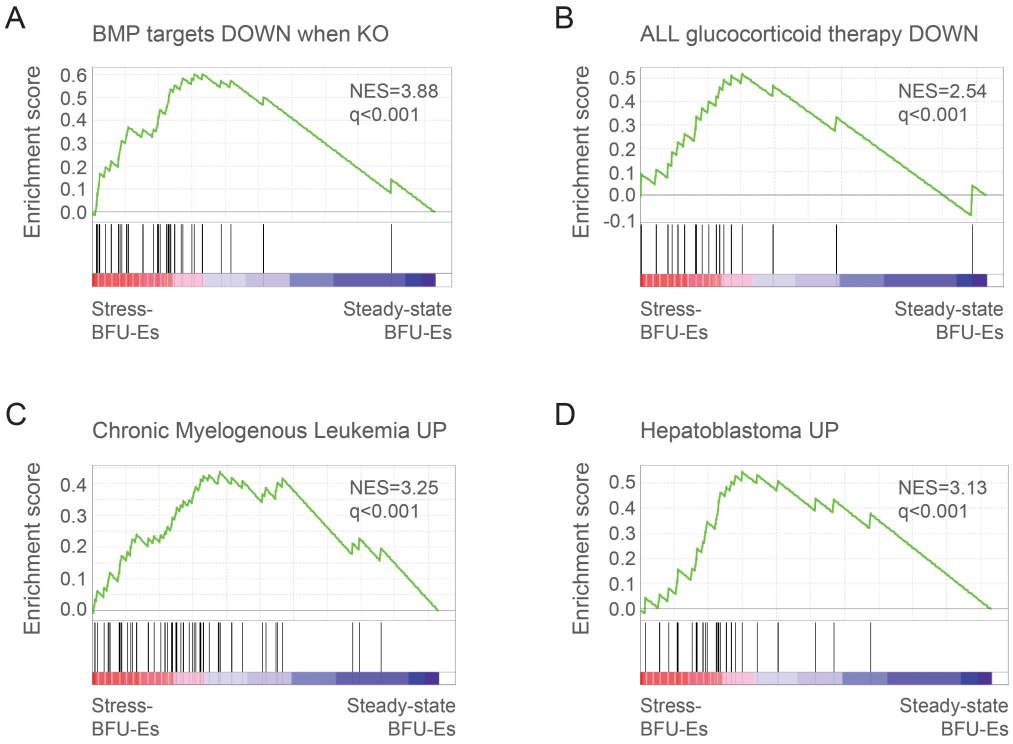

Supplemental Figure 8. GSEA of differentially expressed genes between stress- and steady-state BFU-Es.

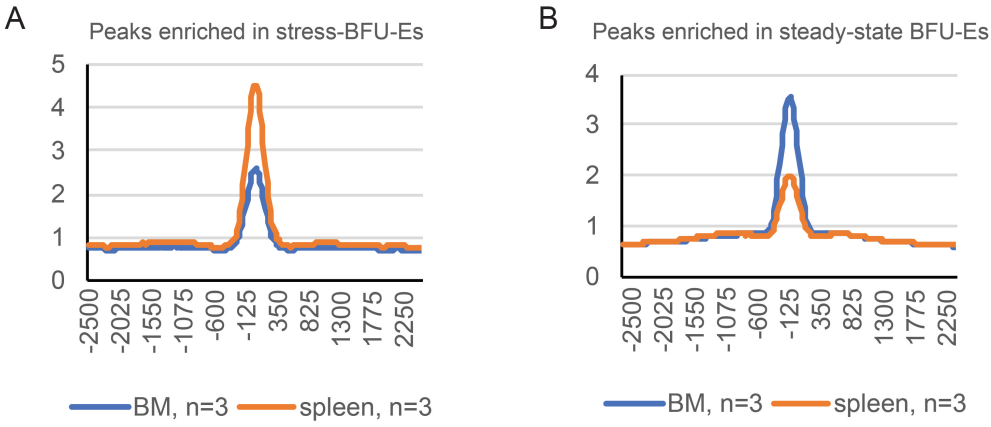

Supplemental Figure 9. ATAC peak enrichment in stress- and steady-state BFU-Es.

Supplemental Figure Legends

Supplemental Figure 1. Identification of CD9 as a novel marker of stress BFU-Es. (A) Strategy for selecting novel markers based on gene expression levels in E14.5-15.5 fetal liver BFU-E, CFU-E, and Ter119+ cells using RNA sequencing as previously described[1]. The table displays surface markers with 10 times higher expression (RPKM) values in mature Ter119+ cells than BFU-Es for negative selection (top), and 10 times higher in BFU-Es than CFU-Es for positive selection (bottom). (B-C) FACS profiles of novel markers within lineage- Kit+ cells for (B) negative selection using CD24a and (C) positive selection for stress-BFU-Es. Only CD9 could further fractionate lineage- Kit+ CD71/CD24a low CD150+ cells.

Supplemental Figure 2. CD133 expression does not overlap with CD150+, and does not mark stress BFU-E potential. (A) FACS analysis of lineage- cKit+ CD71low CD24low cells reveals that CD133 does not overlap with CD150 or Sca1, but does have some overlap with CD9. (B) CD133+ cells mainly give rise to mature erythroid colonies.

Supplemental Figure 3. In vivo repopulation potential and kinetics of isolated splenic day 8 stress progenitors in peripheral blood. (A) Table displaying the overall composition (not within KuO+) of whole peripheral blood (PB) over time after transplantation of different CD150+ stress progenitor populations (RBCs: red blood cells). (B-D) Differentiation potential of transplanted KuO+ FACS-sorted progenitors to contribute to (B) reticulocytes (displayed as total percentage of whole PB, 1 week data expanded in left corner), (C) B-cells (B220+) and (D) T-cells (CD4/CD8+) in PB (lysed RBCs) as determined by FACS (n=6 at 1-2w and n=3 at 4w). Data displayed as average +/- SEM. P values are based on Two- way ANOVA followed by Tukey's multiple comparisons test. **P≤0.01, ****P≤0.0001.

Supplemental Figure 4. In vivo repopulation potential and kinetics of early progenitors in spleen. Potential of transplanted KuO+ FACS-sorted progenitors to contribute to (A) erythroid cells (Ter119+, p≤0.05 sCFU-Es vs sBFU-Es at 2w), (B) the megakaryocytic lineage (CD41+, p≤0.01 sCFU-Es vs sMPPs at 2w), (C) myeloid cells (Gr1+), (D) B-cells (B220+) and (E) T-cells (CD4/CD8+, p≤0.001 sCFU-Es vs sMPPs and sBFU-Es vs sMPPs at 4w) in spleen, as determined by FACS (n=6 at 1-2w and n=3 at 4w). Data displayed as

average +/- SEM. P values are based on Two-way ANOVA followed by Tukey's multiple comparisons test.

Supplemental Figure 5. In vivo repopulation potential and kinetics of early progenitors in bone marrow. Potential of transplanted KuO+ FACS-sorted progenitors to contribute to (A) erythroid cells (Ter119+, $p \leq 0.01$ sCFU-Es vs sMPPs and sBFU-Es vs sMPPs at 4w), (B) the megakaryocytic lineage (CD41+), (C) myeloid cells (Gr1+), (D) B-cells (B220+) and (E) T-cells (CD4/CD8+) in bone marrow (BM), as determined by FACS (n=6 at 1-2w and n=3 at 4w). Data displayed as average +/- SEM. P values are based on Two-way ANOVA followed by Tukey's multiple comparisons test.

Supplemental Figure 6. Splenic stress progenitors map closely with their steady-state bone marrow counterparts. (A) SPRING plots by Tusi et al., outlining their single cell RNA seq data from Kit+ bone marrow cells, highlighting the distribution of erythroid and megakaryocytic cells, and the distribution of cells expressing CD24a, CD150 and CD9 using software available at https://kleintools.hms.harvard.edu/paper_websites/tusi_et_al/ [13]. (B) Gene profiles of splenic stress progenitor populations (sMPPs; CD150+CD9+Sca1+, sBFU-Es; CD150+CD9+Sca1- and sCFU-Es; CD150+CD9-, see Figure 3) were mapped to published lists of genes enriched in and unique for different Kit+CD55+ bone marrow steady-state erythroid branch progenitor populations based on CD49f, CD105, CD71, CD41 and CD150 expression (P1; erythroid-committed, P2; mostly erythroid-committed and P5; erythroid- biased oligo- and multipotent cells, see previously described methods for gating[13] and https://kleintools.hms.harvard.edu/tools/springViewer_1_6_dev.html?datasets/mouse_HPCs/facs_p1-p5/full for enriched genes lists). This demonstrated that sCFU-Es mapped closest to more mature P1 and P2, whereas the more primitive sBFU-Es and sMPPs mapped with the erythroid-biased oligopotent and multipotent P5 population, verifying a transcriptional overlap between erythroid steady-state and stress progenitors.

Supplemental Figure 7. Only low levels of BFU-E-forming progenitors are found in the spleen during steady-state. (A) Gating strategy and (B) colony forming potential of steady-state spleen progenitors based on CD150/CD9/Sca1 expression, revealing that CD150+CD9+ cells sorted from steady-state spleens only contain low levels of BFU-E-forming progenitors.

All cells were incubated in 4% O2, and scored on day4 (CFU-Es) or day7-8 (BFU-Es). Data displayed as average ± SEM, n.d; not detectable.

Supplemental Figure 8. GSEA of differentially expressed genes between stress- and steady-state BFU-Es. Preranked gene set enrichment analysis (GSEA) of differentially expressed genes (cut off FDR: -log10 of 2 and log2fold change of 0.58, ranked on fold change) in stress-BFU-Es vs steady-state BFU-Es, as outlined in Figure 5. Results for (A) BMP targets DOWN when KO (genes down-regulated in uterus upon knockout of BMP2[14]), (B) ALL glucocorticoid therapy DOWN (genes down-regulated in acute lymphoblastic leukemia blasts after 1 week of treatment with glucocorticoids[15]), (C) Chronic Myelogenous Leukemia UP (genes up-regulated in CD34+ cells isolated from bone marrow of chronic myelogenous leukemia patients, compared to those from normal donors[16]) and (D) Hepatoblastoma UP (genes up-regulated in a highly proliferating immature fetal-like subtype of hepatoblastoma samples, "rC2", compared to those in a more mature subtype, "rC1"[17]) gene sets are shown together with normalized enrichment scores (NES) and FDR adjusted q-values (q).

Supplemental Figure 9. ATAC peak enrichment in stress- and steady-state BFU-Es. Verification of enrichment of ATAC peaks enriched in (A) stress-BFU-Es and (B) steady-state BFU-Es respectively. Mean ATAC-seq signal (merged from triplicates) was plotted on stress and steady-state enriched ATAC peaks (Figure 5) using annotatepeaks.pl with the options -size 5000 and -hist 25 using HOMER[4].

Supplemental Table Legends

Supplemental Table 1. RNA-seq of stress-progenitor populations. The spreadsheet contains information about the raw data processing pipeline from RNA-sequencing of FACS sorted stress-progenitor populations (n=3), as well as gene lists generated from unsupervised clustering of RPKM normalized data on genes with a significantly different expression between any of the samples (FDR<0.05, log2FoldChange>0.58, see *Methods* for details). RefSeq accession numbers and gene symbols are shown for each gene list.

Supplemental Table 2. RNA-seq of stress- and steady-state BFU-Es. The spreadsheet contains information about the raw data processing pipeline from RNA-sequencing of FACS sorted BFU-Es from steady-state bone marrow (ssBFU-Es) and day8 stressed spleens (sBFU-Es) respectively (n=3), as well as a list of differentially expressed genes between these two populations (-log10FDR>2, log2FoldChange>0.58, see *Methods* for details*)*. RefSeq accession numbers, gene symbols, log2 Fold Change (sBFU-Es/ssBFU-Es) and -log10 FDR (False Discovery Rate) values are shown in the gene list.

References

1. Flygare J, Rayon Estrada V, Shin C, Gupta S, Lodish HF. HIF-1 {alpha} synergizes with glucocorticoids to promote BFU-E progenitor self-renewal. Blood. 2011;
2. Edgar R, Domrachev M, Lash AE. Gene Expression Omnibus: NCBI gene expression and hybridization array data repository. Nucleic Acids Res. 2002;30(1):207-210.
3. Dobin A, Davis CA, Schlesinger F, et al. STAR: ultrafast universal RNA-seq aligner. Bioinformatics. 2013;29(1):15-21.
4. Heinz S, Benner C, Spann N, et al. Simple combinations of lineage-determining transcription factors prime cis-regulatory elements required for macrophage and B cell identities. Mol Cell. 2010;38(4):576-589.
5. Love MI, Huber W, Anders S. Moderated estimation of fold change and dispersion for RNA-seq data with DESeq2. Genome Biol. 2014;15(12):550.
6. de Hoon MJ, Imoto S, Nolan J, Miyano S. Open source clustering software. Bioinformatics. 2004;20(9):1453-1454.
7. Saldanha AJ. Java Treeview--extensible visualization of microarray data. Bioinformatics. 2004;20(17):3246-3248.
8. Subramanian A, Tamayo P, Mootha VK, et al. Gene set enrichment analysis: a knowledge-based approach for interpreting genome-wide expression profiles. Proc Natl Acad Sci U S A. 2005;102(43):15545-15550.
9. Liberzon A, Subramanian A, Pinchback R, Thorvaldsdottir H, Tamayo P, Mesirov JP. Molecular signatures database (MSigDB) 3.0. Bioinformatics. 2011;27(12):1739-1740.
10. Mootha VK, Lindgren CM, Eriksson KF, et al. PGC-1alpha-responsive genes involved in oxidative phosphorylation are coordinately downregulated in human diabetes. Nat Genet. 2003;34(3):267-273.
11. Buenrostro JD, Giresi PG, Zaba LC, Chang HY, Greenleaf WJ. Transposition of native chromatin for fast and sensitive epigenomic profiling of open chromatin, DNA-binding proteins and nucleosome position. Nat Methods. 2013;10(12):1213-1218.
12. Langmead B, Trapnell C, Pop M, Salzberg SL. Ultrafast and memory-efficient alignment of short DNA sequences to the human genome. Genome Biol. 2009;10(3):R25.
13. Tusi BK, Wolock SL, Weinreb C, et al. Population snapshots predict early haematopoietic and erythroid hierarchies. Nature. 2018;555(7694):54-60.
14. Lee KY, Jeong JW, Wang J, et al. Bmp2 is critical for the murine uterine decidual response. Mol Cell Biol. 2007;27(15):5468-5478.
15. Rhein P, Scheid S, Ratei R, et al. Gene expression shift towards normal B cells, decreased proliferative capacity and distinct surface receptors characterize leukemic blasts persisting during induction therapy in childhood acute lymphoblastic leukemia. Leukemia. 2007;21(5):897-905.
16. Diaz-Blanco E, Bruns I, Neumann F, et al. Molecular signature of CD34(+) hematopoietic stem and progenitor cells of patients with CML in chronic phase. Leukemia. 2007;21(3):494-504.
17. Cairo S, Armengol C, De Reynies A, et al. Hepatic stem-like phenotype and interplay of Wnt/beta-catenin and Myc signaling in aggressive childhood liver cancer. Cancer Cell. 2008;14(6):471-484.